

## **Integrated DSP Control and Image Acquisition System for Measuring Monochromatic Aberrations in Human Eyes**

**P. Sulisz, M. J. Collins, B. Davis and D. R. Iskander**

Contact Lens and Visual Optics Laboratory, Centre for Eye Research,  
Queensland University of Technology  
Victoria Park Rd, Kelvin Grove 4059, Australia

### **ABSTRACT**

The monochromatic aberrations of the human eye limit visual performance to varying degrees. An aberroscope or a Hartman-Shack sensor can measure the total aberrations of the human eye. The aberroscope that is currently being developed at the Centre for Eye Research consists of a grid pattern that is projected on the eye through a specially designed optical system and a camera that records the resulting grid image from the retina. We propose the development of an integrated DSP system that would simultaneously control the projected grid pattern and capture the retinal images. Also, we derive a detection scheme for calculating the centroids of the retinal grid pattern. These centroids are used to determine the wavefront aberration error function of the human eye. The ability to rapidly acquire multiple patterns/images increases the accuracy of the monochromatic aberration estimates.

### **I INTRODUCTION**

The monochromatic aberration is defined as a defect of an optical system occurring for a single wavelength of light. For the human eye, this wavelength is often chosen to be  $\lambda=555\text{nm}$ . Most common monochromatic aberrations of the eye include defocus, spherical aberration and astigmatism.

In the past, several techniques have been used to measure monochromatic aberrations. Some of the most eye aberration measurements were performed Howland & Howland [1] whose experiments made use of a modified aberroscope system first developed by Tscherning [2]. The Howland's technique required the subject to view a source of an intercalated grid and observe a shadow image of the grid. The subject was then asked to draw what they saw. The distortions of the grid image were quantitatively related to the wavefront aberrations of the eye. These aberrations were then analysed by fitting a two-dimensional Taylor polynomial series to the data.

Walsh and Charman [3] subsequently modified the apparatus proposed in [2]. An ophthalmoscopic arrangement was utilised to directly photograph the grid image projected on the retina. The photographs were then analysed to derive the wavefront aberrations. The use of photography enabled the elimination of the subjects' free-hand sketch as a data source, resulting in an increase in accuracy of results. Collins and Atchison [4,5] further improved the aberroscope technique by using a stimulus system, which allowed the subjects' accommodation (focus level) to be varied.

However, there exist several drawbacks associated with the current aberroscope techniques. Errors may be introduced throughout different stages of the experiment. For instance, automatically captured images still require manual calculations and analysis of data rendering this technique inefficient. The researcher also needs to verify that the subjects' vision is centred on the fixation target before capturing the image. Consequently this may lead to a considerable probability of incorrect captures due to small fluctuations that may arise from the subjects inability to stay fixated for a long duration of time (in comparison to the number of captures required). This issue has a particular significance when measuring monochromatic aberrations in children's eyes.

In previous experiments, the grid (produced in photographic film) that was projected could not be altered in real-time. Therefore, the region of interest was fixed and the produced aberration data was always mapped to the same points on the retina. It was not feasible to gather and analyse data that lie in between the fixed grid points. An alternative approach is to use a set of grid patterns mounted on a carousel. Recently, the team at the Centre for Eye Research has proposed a prototype aberroscope system in which a carousel with several film grid patterns is used. A stepper motor drives the carousel. The system uses two computers, one to control the motor and the second to capture retinal images from a CCD camera. This system is problematic through the use of two software

systems that reside on separate machines and require different operating systems. The image capture system provides simple capture functionality. Images still require to be printed before analysis, producing no significant advantage over previous photographic techniques.

We propose the development of an integrated DSP system that will combine the functionality of the two previously separate systems. This improved system will also apply image-processing techniques to enhance the captured images and accommodate the use of efficient morphological techniques to detect the centroids in the retinal image. The location of the centroids provides a means for estimating the monochromatic aberrations.

## II THE ABERROSCOPE TECHNIQUE

The apparatus consists of a light source, a combination of lens and filter configurations, the aberroscope, beam splitter and a CCD camera as shown in Figure 1.

The light source is a 0.5mm near infrared laser ( $\lambda = 780\text{nm}$ ). The laser beam is passed through a 1.0 N.D. filter and onto the aberroscope grid system. This system consists of a  $-5\text{D}\times 135$  degree plano-cylinder corrective lens, a film grid mounted on a carousel, and a  $+5\text{D}\times 45$  degree plano-cylinder lens. The laser light projects the grid pattern image through a 70/30% reflecting/transmitting beam splitter. The grid image on the retina is then photographed using the CCD camera. The subject is positioned in a headrest affixed to the experimental bench. A stimulus system is used to maintain subject's fixation throughout the duration of image capture.

The laser light intensity is measured to ensure safe operating levels while the projected grid is aligned prior to image capture through experimenter and subject interaction. Once these preliminaries are successfully completed, the computer-based control system is used to manage grid image capture. Analysis of the captured images follows techniques previously described. The distortions in the grid points are closely related to the derived wavefront aberrations, as described in [1]. This relationship warrants the determination of the centroids in the captured grid images.

The wavefront aberration can be modelled by a two-dimensional Taylor series expansion as:

$$W(x, y) = A + Bx + Cy + Dx^2 + Exy + Fy^2 + Gx^3 + Hx^2y + Ixy^2 + Jy^3 + Kx^4 + Lx^3y + Mx^2y^2 + Nxy^3 + Oy^4 + \dots + \epsilon$$

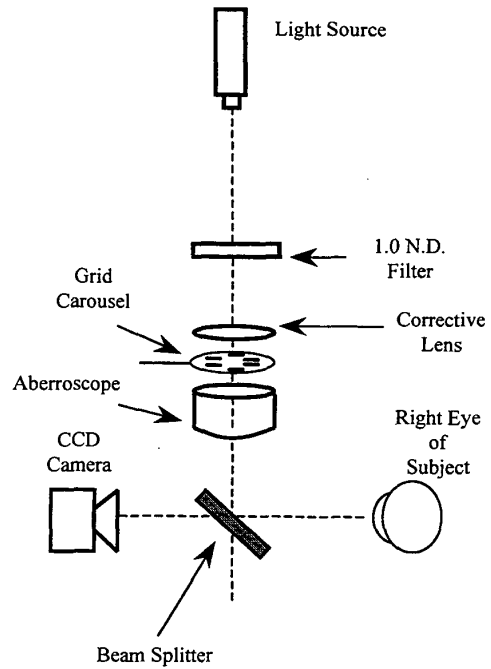


**Figure 1 - Aberroscope Apparatus.**

where  $(x, y)$  are the coordinates in the pupil (mm), its center being the origin of the wavefront and  $\epsilon$  represents the measuring error. The preferred convention models the positive wavefront aberration ( $W$ ) towards the subject, positive- $x$  being towards the subject's right and positive- $y$  upward. In terms of coefficients of the Taylor series,  $A$  describes a shift of the entire wavefront along the  $z$ -axis,  $Bx$  and  $Cy$  correspond to the horizontal and vertical prism components of common spectacle prescriptions, while  $Dx^2$ ,  $Exy$ , and  $Fy^2$  correspond to the sphero-cylindrical components of the prescription. The terms with coefficients  $G-J$  relate to third-order aberrations, and coefficients  $K-O$  relate to fourth-order aberrations respectively. These aberrations produced in the third and fourth-orders cannot be corrected with conventional spectacle lens. To simplify calculations, it is convenient to discard the earlier terms of the series, providing a means of comparing the wavefront aberration of the "corrected" eye with an ideal, flat, reference "sphere" at the cornea.

The distortions in the grid image may be described as two-dimensional displacements of the coordinates of the projected grid intersection points  $(x', y')$ . These displacements designated  $dx'$  and  $dy'$  are described as:

$$dx' = f'(\partial W / \partial y) \quad \text{and} \quad dy' = f'(\partial W / \partial x),$$

where  $f'$  is the second (posterior) focal length of the eye and the partial derivatives of the wavefront aberration with respect to  $x$  and  $y$  are  $\partial W/\partial x$  and  $\partial W/\partial y$ . The displacements are normalised by the spacing of undistorted grid, as:

$$\text{Spacing at Retina} = Cl \times Sp \times f'$$

where  $Cl$  is the power of the crossed-cylinder lens (5D) and  $Sp$  is the actual grid spacing. The normalised displacements become:

$$X = dx'/x' = (\partial W/\partial y) / (Cl \times Sp)$$

$$Y = dy'/y' = (\partial W/\partial x) / (Cl \times Sp).$$

Therefore, corresponding wavefront slopes are:

$$\partial W/\partial y = Cl \times Sp \times Y$$

$$\partial W/\partial x = Cl \times Sp \times X.$$

The resulting matrices represent the surface derivatives sampled at regular intervals. Thus, it is more appropriate to use some set of discrete orthogonal basis functions, such as Zernike polynomials [6], for modelling the wavefront aberration. There exist relationships between the Zernike coefficients and Taylor series coefficients. However, it is more appropriate, from the estimation point of view, to transform the displacements  $dx'$  and  $dy'$  into polar coordinates and use the Zernike polynomials throughout the analysis [3].

### III INTEGRATED CONTROL SYSTEM

The integrated computer-based system comprises of four sub-systems: the input, image processing, data analysis, and output system, as shown in Figure 2.

The output system controls the grid projection functionality. The underlying software for this system provides a means of choosing the required grid geometry. The carousel is controlled via a DSP board. The input system performs the capture of the grid images projected on the retina via a low-light CCD camera. Another DSP card acquires images from this camera at a user-specified frequency. These images are input into the software system for image processing and analysis of data.

The captured images are initially enhanced within the image processing sub-system. The enhanced images are further morphologically processed to allow centroid detection. The resultant data is input to the data analysis sub-system, which performs all mathematical calculations

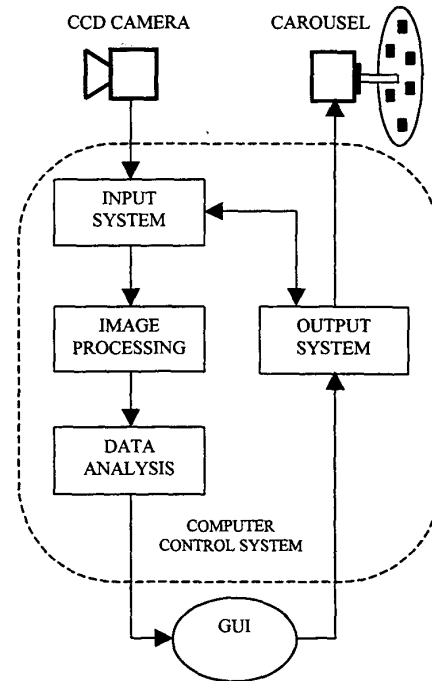


Figure 2 – Computer based control system.

required in determining the monochromatic higher-order aberrations. The input and output systems are synchronised to provide the ability for multiple pattern/image pair capture.

### IV IMAGE PROCESSING AND CENTROID DETECTION

The image processing system endeavours to significantly enhance the input image in order to extract the centroid location data. An example of a projected grid is shown in Figure 3(a).

The captured image from the right eye of one of the authors (subject BD), as shown in Figure 3(b), needs to be pre-processed to qualify the use of morphological operations. This process utilises thresholding and window convolution techniques to identify the approximate regions of interest. First, an appropriate greyscale threshold is applied to condition the image eliminating areas of lower intensity (noise). Then, a circular window kernel is convolved with the image ensuring that the majority of unwanted points are discarded, highlighting important areas of intensity. A priori knowledge of the original grid point size is used as the radius of the circular kernel. The resulting image is shown in Figure 3(c).

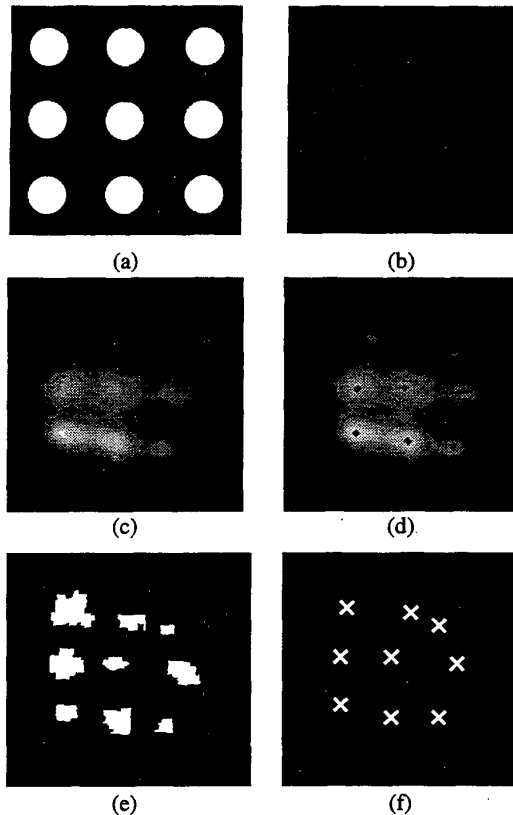


**Figure 3 - Grid image processing and determination of centroids: (a) the original image, (b) the captured image from the right eye of one of the authors (subject BD), (c) preprocessed image, (d) location of regional maxima, (e) watershed partitioning and filled, (f) centroid detection.**

Care is taken to ensure that the size of the image is retained throughout all operations to minimise induced errors in centroid detection. The processed image size is validated after all convolution operations and cropped accordingly. The centroids of the grid image points are determined through a sequence of morphological operations, which segment the image and define the local regions of interest. First, the pre-processed image is further filtered with an alternating sequential filter which uses a  $3 \times 3$  kernel (cross-shaped) to perform iterative morphological opening and closing. The resulting image, together with the  $3 \times 3$  kernel, is utilised in the detection of regional maxima. The resulting coordinates of regional maxima are shown superimposed on the image in the Figure 3 (d).

Then, the Watershed Transform is applied to morphologically segment the image [7]. The algorithm used creates a secondary image which reveals the regional boundaries according to the connectivity of the pixel's with the  $3 \times 3$  (cross shaped) kernel. The boundaries of the watershed transformation are then subsequently filled, as shown in Figure 3 (e), and an iterative shrinking procedure is applied to determine the centroids (single pixels). In Figure 3 (f), for illustrative purposes, the position of the centroids are depicted by crosses .

## V CONCLUSIONS

We have proposed the development of a computer-based system for measuring the monochromatic aberrations of the human eye. The system constitutes of hardware (DSP boards) and software (C/C++) as well as the methodology for detecting the centroids in the retinal grid image. The detection of the centroids in the pre-processed retinal image has been achieved via a set of morphological operations including segmentation of regions of local maxima, watershed transformation, and filling and shrinking transformations. The proposed system may lead in future to a commercially available instrument that will have various applications in vision science, the optical industry and clinically. The prototype could be used as adjunct to clinical instruments, which measure ocular aberrations or corneal topography/aberrations of the eye.

## REFERENCES

1. H. C. Howland and B. Howland, A subjective method for the measurement of monochromatic aberrations of the eye. *J. Opt. Soc. Am.*, 67, pp. 1508-1518, 1977.
2. M Tscherning, *Physiological Optics*, Keystone, Phil., 1900.
3. G. Walsh, and W. N. Charman, Measurement of the axial wavefront aberrations of the human eye. *Ophthalm. Physiol. Opt.*, 5(1), pp. 23-31, 1985.
4. D. A. Atchison, M. J. Collins, C. F. Wildsoet, J. Christensen and M. D. Waterworth, Measurement of monochromatic ocular aberrations of human eyes as a function of accommodation by the Howland aberroscope technique. *Vision Res.* 35(3), pp. 313-323, 1995.
5. M. J. Collins, C. F. Wildsoet, and D. A. Atchison, Monochromatic aberrations and myopia, *Vision Res.* 35(9), pp. 1157-1163, 1995.
6. R. J. Noll, Zernike polynomials and atmospheric turbulence. *J. Opt. Soc. Am.*, 66(3), pp.207-211, 1976.
7. S. Beucher and F. Meyer, The Morphological Approach to Segmentation: The Watershed Transformation. In E.R. Dougherty, editor, *Mathematical Morphology in Image Processing*, Chapter 12, pp. 433-480, Marcel Dekker Inc, New York 1993.